LUND UNIVERSITY

Propagation of transient electromagnetic waves in time-varying media - Direct and inverse scattering problems

Åberg, Ingegerd; Kristensson, Gerhard; Wall, David J. N.

1994

Link to publication

Citation for published version (APA):
Åberg, I., Kristensson, G., & Wall, D. J. N. (1994). *Propagation of transient electromagnetic waves in time-varying media - Direct and inverse scattering problems*. (Technical Report LUTEDX/(TEAT-7030)/1-26/(1994); Vol. TEAT-7030). [Publisher information missing].

Total number of authors:
3

General rights
Unless other specific re-use rights are stated the following general rights apply:
Copyright and moral rights for the publications made accessible in the public portal are retained by the authors and/or other copyright owners and it is a condition of accessing publications that users recognise and abide by the legal requirements associated with these rights.
• Users may download and print one copy of any publication from the public portal for the purpose of private study or research.
• You may not further distribute the material or use it for any profit-making activity or commercial gain
• You may freely distribute the URL identifying the publication in the public portal

Read more about Creative commons licenses: https://creativecommons.org/licenses/

Take down policy
If you believe that this document breaches copyright please contact us providing details, and we will remove access to the work immediately and investigate your claim.

LUND UNIVERSITY

PO Box 117
221 00 Lund
+46 46-222 00 00

CODEN:LUTEDX/(TEAT-7030)/1-26/(1994)

Revision No. 4: November 1994

Propagation of transient electromagnetic waves in time-varying media—Direct and inverse scattering problems

Ingegerd Åberg, Gerhard Kristensson and David J. N. Wall

Department of Electroscience
Electromagnetic Theory
Lund Institute of Technology
Sweden

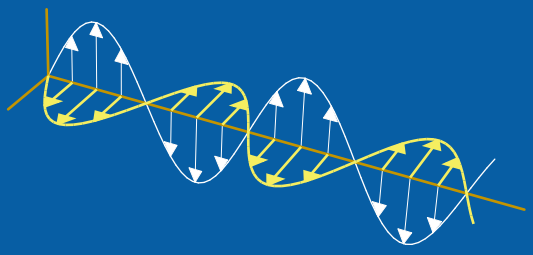

Ingegerd Åberg, Gerhard Kristensson

Department of Electromagnetic Theory
Lund Institute of Technology
P.O. Box 118
SE-221 00 Lund
Sweden

David J. N. Wall

Department of Mathematics
University of Canterbury
Christchurch 1
New Zealand

Editor: Gerhard Kristensson
© Ingegerd Åberg *et al.*, Lund, November 1, 1994

Abstract

Wave propagation of transient electromagnetic waves in time-varying media is considered. The medium, which is assumed to be inhomogeneous and dispersive, lacks invariance under time translations. The spatial variation of the medium is assumed to be in the depth coordinate, i.e., it is stratified. The constitutive relations of the medium is a time integral of a generalized susceptibility kernel and the field. The generalized susceptibility kernel depends on one spatial and two time coordinates. The concept of wave splitting is introduced. The direct and inverse scattering problems are solved by the use of an imbedding or a Green functions approach. The direct and the inverse scattering problems are solved for a homogeneous semi-infinite medium. Explicit algorithms are developed. In this inverse scattering problem, a function depending on two time coordinates is reconstructed. Several numerical computations illustrate the performance of the algorithms.

1 Introduction

During the last decades, an impressive development in the field of inverse scattering problems has occurred. Specifically, several recent conferences have addressed these problems, see e.g., [2, 15, 16]. Many useful algorithms have been developed and interesting new mathematics has been created.

The time domain techniques have been very successful in the solution of the inverse scattering problem. These methods, which are based upon a wave splitting concept in conjunction with imbedding or Green function techniques, have in this context proved to be very efficient. These methods originate from work by Corones, Krueger and co-workers, see Refs. [1, 3, 4, 11]. Several recent results using these methods are collected in Ref. [5], and the interesting progress in the solution of the three-dimensional inverse scattering problem is found in Ref. [17, 18].

The traditional underlying model for wave propagation in general is the wave equation with coefficients that are independent of time. No changes in the material parameters are allowed, i.e., the medium is assumed to be invariant under time translations. The literature on the solution of the inverse scattering problem for a non-stationary medium is sparse, see e.g. [12–14]. The inverse scattering problem for the time-invariant wave equation using time domain techniques has been studied extensively, and several numerical algorithms have been suggested in the literature. The most relevant references, for the generalizations of this problem presented in this paper, are Refs. [6–10].

In this paper a wider class of underlying differential equations is analyzed. The properties of the medium can change during the scattering experiment. In order to analyze such a situation, the coefficients of the partial differential equation must be time dependent. To deal with these conditions, several new extensions of the existing theory have to be introduced and examined. The concept of wave splitting is introduced and the imbedding and Green function techniques are investigated. The analysis is illustrated with several numerical computations for some simple model problems.

Model problems, where time dependent coefficients occur, can be found in telecommunication problems, e.g., fading and modulation problems. Other interesting fields of applications are found in control theory and linearizations of non-linear electromagnetic effects, such as the Kerr effect. Microwave propagation in ferrites also shows applications that can be modeled with time dependent coefficients.

In Section 2 the prerequisite equations are developed. The wave splitting concept is introduced in Section 3, and the imbedding and Green function approaches are analyzed in Sections 4 and 5, respectively. The homogeneous case is investigated in Section 6 and some numerical illustrations are found in Section 7. The paper ends with three appendices containing additional analysis.

2 Basic equations

In this paper, the Maxwell equations are the underlying differential equations of the analysis. These equations give the dynamics of the electric field $\boldsymbol{E}(\boldsymbol{r},t)$, the magnetic field $\boldsymbol{H}(\boldsymbol{r},t)$, the magnetic induction $\boldsymbol{B}(\boldsymbol{r},t)$ and the electric displacement field $\boldsymbol{D}(\boldsymbol{r},t)$.

$$\begin{cases} \nabla \times \boldsymbol{E}(\boldsymbol{r},t) = -\dfrac{\partial \boldsymbol{B}}{\partial t}(\boldsymbol{r},t) \\ \nabla \times \boldsymbol{H}(\boldsymbol{r},t) = \dfrac{\partial \boldsymbol{D}}{\partial t}(\boldsymbol{r},t) \end{cases} \tag{2.1}$$

All fields in this paper are assumed to be quiescent before a fixed time. This property guarantees that all fields vanish at $t \to -\infty$.

The medium is assumed to be inhomogeneous with respect to depth z and to be non-magnetic. The relevant constitutive relations used in this paper are:

$$\begin{cases} \boldsymbol{D}(\boldsymbol{r},t) = \epsilon_0 \left(\epsilon(z)\boldsymbol{E}(\boldsymbol{r},t) + \displaystyle\int_{-\infty}^{t} \chi(z,t,t')\boldsymbol{E}(\boldsymbol{r},t')\,dt' \right) \\ \boldsymbol{B}(\boldsymbol{r},t) = \mu_0 \boldsymbol{H}(\boldsymbol{r},t) \end{cases} \tag{2.2}$$

Notice that no assumption on invariance to time translations has been made. The properties of the medium can therefore change during the wave propagation, or stated differently; the medium is aging. The permittivity and the permeability of the medium are denoted $\epsilon_0\epsilon(z)$ and μ_0, respectively.

For simplicity, the relative permittivity $\epsilon(z)$ is assumed to be independent of time, continuous everywhere, and constant outside the slab $[0, L]$, see Figure 1. Generalizations to time-varying permittivity will be reported elsewhere. The susceptibility kernel $\chi(z,t,t')$, which models the aging of the medium, is assumed to be zero outside $[0, L]$. Furthermore, $\epsilon(z)$ and $\chi(z,t,t')$ are assumed to be continuously differentiable inside the slab as functions of $z \in (0, L)$ and $\chi(z,t,t')$ is assumed to be twice continuously differentiable as a function of t and once continuously differentiable as a function of t', where $t \geq t'$. It is convenient to extend the domain of definition of $\chi(z,t,t')$ to the region $t < t'$ by letting $\chi(z,t,t') = 0$, when $t < t'$. In this way $\chi(z,t,t')$ is defined for all t and t'.

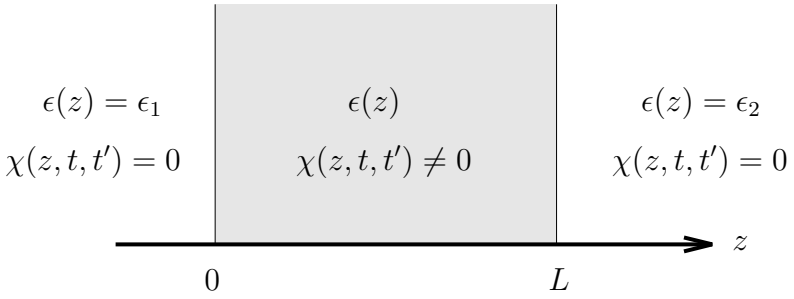

Figure 1: Geometry of the problem.

The Maxwell equations, (2.1), and the constitutive relations, (2.2), combine to

$$\nabla \times (\nabla \times \boldsymbol{E}(\boldsymbol{r},t)) = -\frac{1}{c_0^2}\frac{\partial^2}{\partial t^2}\left(\epsilon(z)\boldsymbol{E}(\boldsymbol{r},t) + \int_{-\infty}^{t} \chi(z,t,t')\boldsymbol{E}(\boldsymbol{r},t')\,dt'\right)$$

The electric field $\boldsymbol{E}$ in this paper is assumed to depend on (z,t) only, and, furthermore, to be transverse to the z-axis. The equation in the electric field then reduces to a generalized scalar wave equation

$$\left(\frac{\partial^2}{\partial z^2} - \frac{\epsilon(z)}{c_0^2}\frac{\partial^2}{\partial t^2} + b(z,t)\frac{\partial}{\partial t} + c(z,t)\right)E(z,t) + \int_{-\infty}^{t} d(z,t,t')E(z,t')\,dt' = 0$$

where the time dependent coefficients are

$$\begin{cases} b(z,t) = -\dfrac{1}{c_0^2}\chi(z,t,t) \\ c(z,t) = -\dfrac{1}{c_0^2}\left(2\dfrac{\partial \chi}{\partial t}\,(z,t,t')|_{t'=t} + \dfrac{\partial \chi}{\partial t'}\,(z,t,t')|_{t'=t}\right) \\ d(z,t,t') = -\dfrac{1}{c_0^2}\dfrac{\partial^2 \chi}{\partial t^2}(z,t,t') \end{cases}$$

This equation is the model equation of this paper.

2.1 Travel time coordinate transformation

In order to obtain a canonical set of equations, a travel time coordinate transformation is introduced. This coordinate transformation is not essential for the analysis, but makes the numerical treatment introduced later in the paper simpler. The transformation is

$$\begin{cases} x(z) = \dfrac{1}{lc_0}\displaystyle\int_0^z \sqrt{\epsilon(z')}\,dz' \\ s = \dfrac{t}{l} \end{cases}$$

where the time constant l is

$$l = \frac{1}{c_0} \int_0^L \sqrt{\epsilon(z)}\, dz$$

This transformation transforms the partial differential equation into the canonical equation.

$$\begin{aligned} u_{xx}(x,s) - u_{ss}(x,s) + A(x)u_x(x,s) + B(x,s)u_s(x,s) \\ + C(x,s)u(x,s) + \int_{-\infty}^{s} D(x,s,s')u(x,s')\, ds' = 0 \end{aligned} \tag{2.3}$$

where

$$u(x,s) = E(z(x), sl)$$

and where the coefficients in the partial differential equation are

$$\begin{cases} A(x) = \dfrac{1}{2}\dfrac{\mathrm{d}}{\mathrm{d}x} \ln \epsilon(z(x)) \\ B(x,s) = -\dfrac{l}{\epsilon(z(x))} \chi(z(x), sl, sl) \\ C(x,s) = -\dfrac{l}{\epsilon(z(x))} \left(2\dfrac{\partial \chi}{\partial s}\, (z(x), sl, s'l)|_{s'=s} + \dfrac{\partial \chi}{\partial s'}\, (z(x), sl, s'l)|_{s'=s} \right) \\ D(x,s,s') = -\dfrac{l}{\epsilon(z(x))} \dfrac{\partial^2 \chi}{\partial s^2} (z(x), sl, s'l) \end{cases} \tag{2.4}$$

Notice that all coefficients, except $A(x)$, are time dependent. It is straightforward to generalize the results below to the case where also the coefficient $A(x)$ is time dependent.

3 Wave splitting

The wave splitting of the fields is introduced to obtain a natural set of dependent coordinates that is adapted to the scattering situation. In free space, i.e., outside the slab, the wave splitting projects out the right- and left-moving parts of the solution, respectively. The concept of wave splitting has also been generalized to three spatial dimensions [17].

Proceeding formally, the wave splitting is defined by the following transformation of the dependent variables [7]:

$$\begin{pmatrix} u^+ \\ u^- \end{pmatrix} = \frac{1}{2} \begin{pmatrix} 1 & -\partial_s^{-1} \\ 1 & \partial_s^{-1} \end{pmatrix} \begin{pmatrix} u(x,s) \\ u_x(x,s) \end{pmatrix}$$

with inverse

$$\begin{pmatrix} u(x,s) \\ u_x(x,s) \end{pmatrix} = \begin{pmatrix} 1 & 1 \\ -\partial_s & \partial_s \end{pmatrix} \begin{pmatrix} u^+ \\ u^- \end{pmatrix}$$

where the anti-derivative ∂_s^{-1} is defined as

$$\partial_s^{-1} f(s) = \int_{-\infty}^{s} f(s')\, ds'$$

The new fields $u^{\pm}(x,s)$ satisfy an hyperbolic partial differential equation equivalent to (2.3). Equation (2.3) and the aforementioned definition of the wave splitting imply that the fields $u^{\pm}(x,s)$ satisfy

$$\frac{\partial}{\partial x}\begin{pmatrix} u^+ \\ u^- \end{pmatrix} = \begin{pmatrix} \alpha & \beta \\ \gamma & \delta \end{pmatrix}\begin{pmatrix} u^+ \\ u^- \end{pmatrix} \tag{3.1}$$

The operators α, β, γ, and δ are

$$\begin{cases} (\alpha f(x,\cdot))(s) = -\dfrac{\partial f}{\partial s}(x,s) - \dfrac{A(x)-B(x,s)}{2} f(x,s) \\ \qquad\qquad + \displaystyle\int_{-\infty}^{s} \mathcal{A}(x,s,s') f(x,s')\, ds' \\ (\beta f(x,\cdot))(s) = \dfrac{A(x)+B(x,s)}{2} f(x,s) + \displaystyle\int_{-\infty}^{s} \mathcal{A}(x,s,s') f(x,s')\, ds' \\ (\gamma f(x,\cdot))(s) = \dfrac{A(x)-B(x,s)}{2} f(x,s) - \displaystyle\int_{-\infty}^{s} \mathcal{A}(x,s,s') f(x,s')\, ds' \\ (\delta f(x,\cdot))(s) = \dfrac{\partial f}{\partial s}(x,s) - \dfrac{A(x)+B(x,s)}{2} f(x,s) \\ \qquad\qquad - \displaystyle\int_{-\infty}^{s} \mathcal{A}(x,s,s') f(x,s')\, ds' \end{cases}$$

where the kernel function $\mathcal{A}(x,s,s')$ is defined as

$$\mathcal{A}(x,s,s') = -\frac{l}{2\epsilon(z(x))}\frac{\partial \chi}{\partial s}(z(x), sl, s'l)$$

4 Imbedding equation

The two new functions $u^{\pm}(x,s)$ that were introduced in the previous section are related to each other. The relationship between $u^{\pm}(x,s)$ is closely associated to the scattering operators of the problem, and can be obtained from Duhamel's principle. For a specific x value this relation can be represented as a time integral

$$u^-(x,s) = \int_{-\infty}^{s} R(x,s,s') u^+(x,s')\, ds' \tag{4.1}$$

The kernel $R(x,s,s')$ can be interpreted as the scattering kernel for a subsection $[x,1]$ of the full physical slab $[0,1]$. The physical scattering problem of the slab $[0,1]$ is therefore imbedded in a one-parameter family of sub-slabs $[x,1]$, where the left end of the slab x varies between 0 and 1. The physical reflection kernel, measured in

an experiment, corresponds to $x = 0$, i.e., $R(0, s, s')$. Note because of time varying coefficients in (3.1), the kernel R is of a more general form than that usually taken.

Similar arguments give the relation between the transmitted field $u^+(1, s)$ and the excitation $u^+(x, s)$. This relation yields the imbedded transmission kernel $T(x, s, s')$.

$$u^+(1, s+1-x) = t(x, 1, s-x)u^+(x, s) + \int_{-\infty}^{s} T(x, s, s')t(x, 1, s'-x)u^+(x, s')\, ds' \quad (4.2)$$

where the attenuation factor $t(x, y, s)$ is

$$t(x, y, s) = \exp\left\{\frac{1}{2}\int_x^y B(x', x'+s) - A(x')\, dx'\right\}$$

Straightforward calculations, using the definition of the reflection kernel in equation (4.1) and the dynamics, (3.1) give the imbedding equation for the reflection kernel $R(x, s, s')$ in the domain $0 < x < 1$, $s > s'$. The result is

$$\begin{aligned}
\frac{\partial R}{\partial x}(x, s, s') &- \frac{\partial R}{\partial s}(x, s, s') + \frac{\partial R}{\partial s'}(x, s, s') = -\mathcal{A}(x, s, s') \\
&- \frac{B(x, s) + B(x, s')}{2} R(x, s, s') \\
&- \int_{s'}^{s} R(x, s, s'')\mathcal{A}(x, s'', s')\, ds'' - \int_{s'}^{s} \mathcal{A}(x, s, s'')R(x, s'', s')\, ds'' \\
&- \int_{s'}^{s} R(x, s, s'')\frac{A(x) + B(x, s'')}{2} R(x, s'', s')\, ds'' \\
&- \int_{s'}^{s} \left\{\int_{s'}^{s''} R(x, s, s'')\mathcal{A}(x, s'', s''')R(x, s''', s')\, ds'''\right\} ds''
\end{aligned} \quad (4.3)$$

with an initial condition

$$R(x, s, s')|_{s'=s} = -\frac{A(x) - B(x, s)}{4} \quad (4.4)$$

and a boundary condition, at $x = 1$ $(s > s')$

$$R(1, s, s') = 0 \quad (4.5)$$

An imbedding equation for the transmission kernel $T(x, s, s')$ can also be derived using similar arguments as above; see Ref. [7] for an imbedding equation in a medium that is invariant under time translations.

The imbedding equation (4.3) has the characteristic direction

$$\hat{\xi} = \frac{\hat{x} - \hat{s} + \hat{s'}}{\sqrt{3}}$$

in the (x, s, s')-space. Standard theory of hyperbolic equations shows that Cauchy data on a surface γ parameterized by

$$\begin{cases} x = f_1(t_1, t_2) \\ s = f_2(t_1, t_2) \\ s' = f_3(t_1, t_2) \end{cases}$$

will give a locally unique solution to the imbedding equation, provided the Jacobian J does not vanish, i.e.,

$$J = \begin{vmatrix} \frac{\partial f_1}{\partial t_1} & \frac{\partial f_2}{\partial t_1} & \frac{\partial f_3}{\partial t_1} \\ \frac{\partial f_1}{\partial t_2} & \frac{\partial f_2}{\partial t_2} & \frac{\partial f_3}{\partial t_2} \\ 1 & -1 & 1 \end{vmatrix} \neq 0$$

Therefore, with the initial data specified on the plane $s' = s$, as in equation (4.4), the problem (4.3) is well-posed.

4.1 Propagation of discontinuity

In this section the propagation of singularity of the reflection kernel is analyzed in greater detail. In particular, an equation defining the finite jump discontinuity of the kernel is derived.

Any finite jump discontinuity in $R(x, s, s')$, that is initiated on the plane $s = s'$, see (4.4), propagates along the characteristic direction $\hat{\xi}$. From the continuity requirements of the susceptibility kernel $\chi(z, t, t')$ mentioned in Section 2, the only finite jump discontinuity in the reflection kernel that can be initiated is at $x = 1$. The direction vector

$$\hat{\tau} = \frac{\hat{s} + \hat{s'}}{\sqrt{2}}$$

together with the characteristic direction $\hat{\xi}$ of the imbedding equation (4.3) span a plane Γ

$$s - s' = 2(1 - x)$$

with normal $\hat{n}$

$$\hat{n} = \frac{2\hat{x} + \hat{s} - \hat{s'}}{\sqrt{6}}$$

The reflection kernel $R(x, s, s')$ is discontinuous across this plane.

The finite jump discontinuity in the reflection $R(x, s, s')$ across the line $s = s'$ is (see (4.4) and (4.5))

$$[R(1, s, s)] = \frac{A(1^-) - B(1^-, s)}{4}$$

where square brackets are used to denote the finite jump discontinuity with respect to the normal $\hat{n}$, i.e.,

$$[R(x, s, s - 2(1 - x))] = R(x^+, s^+, s - 2(1 - x)) - R(x^-, s^-, s - 2(1 - x))$$

If the plane Γ is parameterized as

$$\begin{cases} x = 1 - q \\ s = p + q \\ s' = p - q \end{cases}$$

then the jump discontinuity of the reflection kernel, which is determined by the imbedding equation (4.3), satisfies

$$\frac{\mathrm{d}}{\mathrm{d}q}\left[R(1-q,p+q,p-q)\right] = \frac{B(1-q,p-q)+B(1-q,p+q)}{2}\left[R(1-q,p+q,p-q)\right]$$

The solution to this ordinary differential equation is

$$[R(x,s,s-2(1-x))] = [R(1,s+x-1,s+x-1)]\exp\left\{\int_x^1 h(x,s,x')\,dx'\right\}$$

where

$$h(x,s,x') = \frac{B(x',s+x+x'-2)+B(x',s+x-x')}{2}$$

Specifically, at $x=0$ the finite jump discontinuity of the physical reflection kernel $R(0,s,s')$ after one round trip is

$$\begin{aligned}[R(0,s,s-2)] &= [R(1,s-1,s-1)]\exp\left\{\int_0^1 h(0,s,x')\,dx'\right\} \\ &= \frac{A(1^-)-B(1^-,s-1)}{4}\exp\left\{\frac{1}{2}\int_0^1 \left[B(x',s+x'-2)+B(x',s-x')\right]\,dx'\right\}\end{aligned} \tag{4.6}$$

5 Green functions

The relationship between the split fields $u^{\pm}$ in Section 4 was evaluated at a specific x-value and the reflection kernel $R(x,s,s')$ was interpreted as the reflection kernel for a subslab $[x,1]$ of the physical slab $[0,1]$. This interpretation was performed by the use of an imbedding argument.

In contrast to the analysis presented in the previous section, this section contains an analysis of the relationship between the exterior excitation $u^+(0,s)$ and the internal fields $u^{\pm}(x,s)$ of the physical slab $[0,1]$. The operator that maps the excitation $u^+(0,s)$ to the internal fields $u^{\pm}(x,s)$ has an integral representation. This representation leads to the definition of the Green functions $G^{\pm}(x,s,s')$ of the propagation problem.

By using Duhamel's principle, the explicit representation of the mapping of the excitation $u^+(0,s)$ to the internal fields $u^{\pm}(x,s)$ is obtained.

$$\begin{cases} u^+(x,x+s) = t(0,x,s)u^+(0,s) + \displaystyle\int_{-\infty}^{s} G^+(x,s,s')t(0,x,s')u^+(0,s')\,ds' \\ u^-(x,x+s) = \displaystyle\int_{-\infty}^{s} G^-(x,s,s')t(0,x,s')u^+(0,s')\,ds' \end{cases} \tag{5.1}$$

where, as above, the attenuation factor is defined as

$$t(x,y,s) = \exp\left\{\frac{1}{2}\int_x^y B(x',x'+s)-A(x')\,dx'\right\}$$

The Green functions equations are obtained from the definition of the Green functions, (5.1), and the dynamics of the field $u^{\pm}(x,s)$, see (3.1). The domain of these equations is $0<x<1$, $s>s'$. The equations are

$$\begin{aligned}\frac{\partial G^{+}}{\partial x}(x,s,s') &+ \frac{B(x,x+s')-B(x,x+s)}{2}G^{+}(x,s,s') \\ &- \frac{A(x)+B(x,x+s)}{2}G^{-}(x,s,s') - \mathcal{A}(x,x+s,x+s') \\ &- \int_{s'}^{s}\mathcal{A}(x,x+s,x+s'')\left(G^{+}(x,s'',s')+G^{-}(x,s'',s')\right)\,ds'' = 0\end{aligned} \tag{5.2}$$

and

$$\begin{aligned}\frac{\partial G^{-}}{\partial x}(x,s,s') &- 2\frac{\partial G^{-}}{\partial s}(x,s,s') - \frac{A(x)-B(x,x+s)}{2}G^{+}(x,s,s') \\ &+ \frac{B(x,x+s')+B(x,x+s)}{2}G^{-}(x,s,s') + \mathcal{A}(x,x+s,x+s') \\ &+ \int_{s'}^{s}\mathcal{A}(x,x+s,x+s'')\left(G^{+}(x,s'',s')+G^{-}(x,s'',s')\right)\,ds'' = 0\end{aligned} \tag{5.3}$$

with the initial condition

$$G^{-}(x,s,s')\big|_{s'=s} = -\frac{A(x)-B(x,x+s)}{4} \tag{5.4}$$

The boundary conditions for $G^{\pm}(x,s,s')$ at $x=0$ and $x=1$ are obtained by using the definition of the Green functions $G^{\pm}(x,s,s')$, (5.1), and by a comparison with the definitions of the imbedded scattering kernels $R(x,s,s')$ and $T(x,s,s')$, (4.1) and (4.2). The boundary values at $x=0$ and $x=1$ ($s>s'$) are

$$\begin{cases} G^{+}(1,s,s') = T(0,s,s') \\ G^{-}(1,s,s') = 0 \\ G^{+}(0,s,s') = 0 \\ G^{-}(0,s,s') = R(0,s,s') \end{cases}$$

From the definition of the Green functions $G^{\pm}(x,s,s')$ in (5.1) and the definitions of the imbedded scattering kernels $R(x,s,s')$ and $T(x,s,s')$ in (4.1) and (4.2), it is possible to obtain additional relations between the imbedding kernels $R(x,s,s')$ and $T(x,s,s')$ and the Green functions $G^{\pm}(x,s,s')$. These relations are

$$G^{-}(x,s,s') = R(x,x+s,x+s') + \int_{s'}^{s}R(x,x+s,x+s'')G^{+}(x,s'',s')\,ds''$$

and

$$\begin{aligned}G^{+}(1,s,s') = T(x,x+s,x+s') &+ \frac{1}{t(x,1,s')}\Big\{t(x,1,s)G^{+}(x,s,s') \\ &+ \int_{s'}^{s}T(x,x+s,x+s'')t(x,1,s'')G^{+}(x,s'',s')\,ds''\Big\}\end{aligned}$$

The Green function $G^-(x,s,s')$ has a finite jump discontinuity along the plane Γ

$$s - s' = 2(1-x)$$

The derivation of this discontinuity follows the same line of arguments as for the reflection kernel $R(x,s,s')$ in Section 4.1. The result is

$$\begin{aligned}
&\big[G^-(x,s,s-2(1-x))\big] \\
&= \big[G^-(1,s-2(1-x),s-2(1-x))\big] \exp\left\{\int_x^1 h(x,s,x')\,dx'\right\} \\
&= \frac{A(1^-) - B(1^-,s+2x-1)}{4} \exp\left\{\int_x^1 h(x,s,x')\,dx'\right\}
\end{aligned} \tag{5.5}$$

where

$$h(x,s,x') = \frac{B(x',s+x'-2(1-x)) + B(x',s+2x-x')}{2}$$

This finite jump discontinuity agrees at $x=0$ with the result in (4.6).

6 Homogeneous, semi-infinite medium

In this section the simplifications that occur in a homogeneous, semi-infinite medium are discussed.

6.1 Imbedding equation

For a homogeneous, semi-infinite medium the imbedding equation (4.3) simplifies considerably. In a homogeneous medium $A(x) = 0$ and the x-dependence in all parameters vanishes. Furthermore, the reflection kernel $R(x,s,s')$ is independent of the imbedding parameter x so that the kernel satisfies the following simplified equation ($s > s'$):

$$\begin{aligned}
\frac{\partial R}{\partial s}(s,s') - \frac{\partial R}{\partial s'}(s,s') &= \mathcal{A}(s,s') + \frac{B(s)+B(s')}{2} R(s,s') \\
&+ \int_{s'}^{s} R(s,s'')\mathcal{A}(s'',s')\,ds'' + \int_{s'}^{s} \mathcal{A}(s,s'')R(s'',s')\,ds'' \\
&+ \frac{1}{2}\int_{s'}^{s} R(s,s'')B(s'')R(s'',s')\,ds'' \\
&+ \int_{s'}^{s}\left\{\int_{s'}^{s''} R(s,s'')\mathcal{A}(s'',s''')R(s''',s')\,ds'''\right\} ds''
\end{aligned} \tag{6.1}$$

with an initial condition

$$R(s,s')|_{s'=s} = \frac{B(s)}{4} \tag{6.2}$$

and where the material functions are

$$\begin{cases} B(s) = -\dfrac{l}{\epsilon}\chi(sl, sl) \\ \mathcal{A}(s, s') = -\dfrac{l}{2\epsilon}\dfrac{\partial\chi}{\partial s}(sl, s'l) \end{cases} \tag{6.3}$$

Numerical algorithms for the direct and the inverse scattering problem are easily obtained from the imbedding equation (6.1). For the direct problem, the susceptibility kernel $\chi(sl, sl')$ is known and the problem is to calculate $R(s, s')$ for $0 \le s \le T$, $0 \le s' \le s$ for some specified T. In the inverse problem, $R(s, s')$ is specified for $0 \le s \le T$, $0 \le s' \le s$ and $\chi(sl, sl')$ is to be determined.

Integration along the characteristic of (6.1) gives

$$\begin{aligned} R(s, s') - R(s-h, s'+h) = \int_{s-h}^{s} \Big\{ & \mathcal{A}(\lambda, s'+s-\lambda) \\ & + \frac{B(\lambda) + B(s'+s-\lambda)}{2} R(\lambda, s'+s-\lambda) \\ & + \int_{s'+s-\lambda}^{\lambda} R(\lambda, s'')\mathcal{A}(s'', s'+s-\lambda)\, ds'' \\ & + \int_{s'+s-\lambda}^{\lambda} \mathcal{A}(\lambda, s'')R(s'', s'+s-\lambda)\, ds'' \\ & + \frac{1}{2}\int_{s'+s-\lambda}^{\lambda} R(\lambda, s'')B(s'')R(s'', s'+s-\lambda)\, ds'' \\ & + \int_{s'+s-\lambda}^{\lambda} \left\{ \int_{s'+s-\lambda}^{s''} R(\lambda, s'')\mathcal{A}(s'', s''')R(s''', s'+s-\lambda)\, ds''' \right\} ds'' \Big\} d\lambda \end{aligned}$$

Up to this point, this is an exact result without approximations. This equation is the starting point for the discretization of the imbedding equation.

Define a staggered mesh in the (s, s')-plane, see Figure 2.

$$(s, s') = (2ih + jh, jh), \qquad i = 0, 1, 2, 3, \ldots, \quad j = 0, 1, 2, 3, \ldots$$

and denote by

$$\begin{cases} R_{i,j} = R(ih, jh) \\ \mathcal{A}_{i,j} = \mathcal{A}(ih, jh)\,, \qquad i = 0, 1, 2, 3, \ldots, I, \quad j = 0, 1, 2, 3, \ldots, J \\ B_i = B(ih) \end{cases}$$

the values at the mesh points in the lower half triangle.

Approximate all integrals by the trapezoidal rule. The result of this approximation is

$$\begin{aligned} R_{i,j} - R_{i-1,j+1} = \frac{h}{2}\Big\{ & \mathcal{A}_{i,j} + \mathcal{A}_{i-1,j+1} + \frac{B_i + B_j}{2} R_{i,j} + \frac{B_{i-1} + B_{j+1}}{2} R_{i-1,j+1} \\ & + \mathcal{K}_{i,j} + \mathcal{K}_{i-1,j+1} + \mathcal{L}_{i,j} + \mathcal{L}_{i-1,j+1} + \mathcal{M}_{i,j} + \mathcal{M}_{i-1,j+1} + \mathcal{N}_{i,j} + \mathcal{N}_{i-1,j+1} \Big\} \end{aligned} \tag{6.4}$$

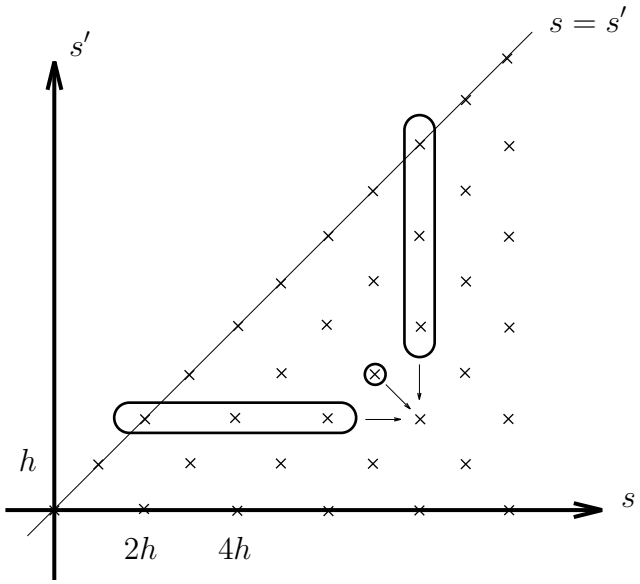

Figure 2: Definition of the mesh in the s-s'-plane and the computational molecule of the algorithms based upon the imbedding equation.

where $i = j+2, j+4, j+6, \ldots, I, \quad j = 0, 1, 2, 3, \ldots, J$ and

$$\begin{cases} \mathcal{K}_{i,j} = 2h \sum\limits_{n=0}^{\frac{i-j}{2}}{}''' R_{i,j+2n} \mathcal{A}_{j+2n,j} \\ \mathcal{L}_{i,j} = 2h \sum\limits_{n=0}^{\frac{i-j}{2}}{}''' \mathcal{A}_{i,j+2n} R_{j+2n,j} \\ \mathcal{M}_{i,j} = h \sum\limits_{n=0}^{\frac{i-j}{2}}{}''' R_{i,j+2n} B_{j+2n} R_{j+2n,j} \\ \mathcal{N}_{i,j} = 2h \sum\limits_{n=0}^{\frac{i-j}{2}}{}''' R_{i,j+2n} \mathcal{L}_{j+2n,j} \end{cases}$$

and for $i = j$ these expressions are

$$\begin{cases} \mathcal{K}_{i,i} = 0 \\ \mathcal{L}_{i,i} = 0 \\ \mathcal{M}_{i,i} = 0 \\ \mathcal{N}_{i,i} = 0 \end{cases}$$

Note that $i - j$ always is an even integer in this algorithm, and the triple prime on the summation symbols signifies that first and last terms in the summation are to

be halved. The initial values of $R_{i,j}$ are

$$R_{i,i} = \frac{B_i}{4}, \quad i = 0, 1, 2, 3, \ldots, I$$

The local truncation error made in (6.4) is of order $O(h^3)$.

6.1.1 Direct algorithm

The direct algorithm requires $R_{i,j}$ to be calculated diagonally from left to right from the diagonal line $s = s'$. This leads to an *implicit* algorithm in (6.4). However, $R_{i,j}$ may be eliminated on the right-hand-side of (6.4) to $O(h^3)$ so yielding the following *explicit* form of the algorithm. Note for sufficiently small step size h, this explicit algorithm is always possible.

$$\begin{aligned} R_{i,j} = \frac{1}{N_{i,j}}\Big\{ & R_{i-1,j+1} + \frac{h}{2}\Big[\mathcal{A}_{i,j} + \mathcal{A}_{i-1,j+1} + \frac{B_{i-1}+B_{j+1}}{2} R_{i-1,j+1} \\ & + \mathcal{K}'_{i,j} + \mathcal{K}_{i-1,j+1} + \mathcal{L}'_{i,j} + \mathcal{L}_{i-1,j+1} + \mathcal{M}'_{i,j} + \mathcal{M}_{i-1,j+1} + \mathcal{N}'_{i,j} + \mathcal{N}_{i-1,j+1}\Big]\Big\} \end{aligned} \tag{6.5}$$

where $i = j+2, j+4, j+6, \ldots, I, \quad j = 0, 1, 2, 3, \ldots, J$. The denominator $N_{i,j}$ is

$$N_{i,j} = 1 - \frac{h}{2}\frac{B_i + B_j}{2} - \frac{h^2}{2}\left(\mathcal{A}_{i,i} + \mathcal{A}_{j,j}\right) - \frac{h^2}{16}\left(B_j^2 + B_i^2\right) + O(h^3)$$

and the truncated sums are

$$\begin{cases} \mathcal{K}'_{i,j} = 2h \sum\limits_{n=1}^{\frac{i-j}{2}}{}'' R_{i,j+2n}\mathcal{A}_{j+2n,j} \\ \mathcal{L}'_{i,j} = 2h \sum\limits_{n=0}^{\frac{i-j-2}{2}}{}' \mathcal{A}_{i,j+2n} R_{j+2n,j} \\ \mathcal{M}'_{i,j} = h \sum\limits_{n=1}^{\frac{i-j-2}{2}} R_{i,j+2n} B_{j+2n} R_{j+2n,j} \\ \mathcal{N}'_{i,j} = 2h \sum\limits_{n=1}^{\frac{i-j-2}{2}} R_{i,j+2n}\mathcal{L}_{j+2n,j} + hR_{i,i}\mathcal{L}'_{i,j} \end{cases}$$

The single and double primes on the summation symbols signify respectively, that either the first or last term in the summation is to be halved.

The starting values of the direct algorithm are

$$R_{i,i} = \frac{B_i}{4}, \quad i = 0, 1, 2, 3, \ldots, I$$

The computations in (6.5) proceed from the diagonal $i = j$ in the direction away from the diagonal; computing $R_{i,j}$ in each subdiagonal $i - j = 2n$, $n = 1, 2, \ldots$ sequentially, from bottom to top. The computations that illustrate this algorithm in Section 7 are limited to the square $0 \le s, s' \le 2$ for practical reasons.

6.1.2 Inverse algorithm

The inverse algorithm based upon the discretized imbedding equation, see (6.4), is obtained in a similar way to the direct problem. In the inverse algorithm the (discretized) values of the reflection kernel $R(s,s')$ are assumed to be known from a scattering experiment. The goal in the inverse algorithms is to retrieve the function $\mathcal{A}_{i,j}$. The function $B(s)$ is easily recovered from the diagonal values of $R(s,s')$, see (6.2), as

$$B_i = 4R_{i,i}, \quad i = 0,1,2,3,\ldots,I$$

The functions $R(s,s')$ and $B(s)$ are therefore known at all relevant mesh points in the s-s'-plane.

From the discretized version of the imbedding equation, (6.4), it is straightforward to make the following rearrangement of terms.

$$\mathcal{A}_{i,j} = \frac{1}{N'_{i,j}}\Big\{\frac{2}{h}\left(R_{i,j} - R_{i-1,j+1}\right) - \mathcal{A}_{i-1,j+1} - \frac{B_i + B_j}{2}R_{i,j} - \frac{B_{i-1} + B_{j+1}}{2}R_{i-1,j+1}$$
$$- \mathcal{K}''_{i,j} - \mathcal{K}_{i-1,j+1} - \mathcal{L}''_{i,j} - \mathcal{L}_{i-1,j+1} - \mathcal{M}_{i,j} - \mathcal{M}_{i-1,j+1} - \mathcal{N}''_{i,j} - \mathcal{N}_{i-1,j+1}\Big\} \tag{6.6}$$

where $i = j+2, j+4, j+6, \ldots, I, \quad j = 0,1,2,3,\ldots,J$. The denominator $N_{i,j}$ in the inverse algorithm is

$$N'_{i,j} = 1 + \frac{h}{2}\frac{B_i + B_j}{2} + \frac{h^2}{16}B_iB_j$$

and the truncated sums are

$$\begin{cases} \mathcal{K}''_{i,j} = 2h\sum\limits_{n=0}^{\frac{i-j-2}{2}}{}' R_{i,j+2n}\mathcal{A}_{j+2n,j} \\ \mathcal{L}''_{i,j} = 2h\sum\limits_{n=1}^{\frac{i-j-2}{2}}{}'' \mathcal{A}_{i,j+2n}R_{j+2n,j} \\ \mathcal{N}''_{i,j} = 2h\sum\limits_{n=1}^{\frac{i-j-2}{2}} R_{i,j+2n}\mathcal{L}_{j+2n,j} + hR_{i,i}\mathcal{L}''_{i,j} \end{cases}$$

The starting values of $\mathcal{A}(s,s')$ on the diagonal $s = s'$ are obtained by evaluating the imbedding equation (6.1) at $s = s'$. The result is

$$\mathcal{A}(s,s) = \frac{\partial R}{\partial s}(s,s')\Big|_{s=s'} - \frac{\partial R}{\partial s'}(s,s')\Big|_{s=s'} - \frac{1}{4}B^2(s)$$

The computations in the inverse algorithm proceed from the diagonal $i = j$ in a downward direction; computing $\mathcal{A}_{i,j}$ in each subdiagonal $i - j = 2n$, $n = 1,2,\ldots$ sequentially, from bottom to top. The computations presented in Section 7 are limited to the square $0 \le s, s' \le 2$ for convenience.

Finally, the susceptibility kernel $\chi(sl, s'l)$ is obtained by numerical integration of $\mathcal{A}(s, s')$, see (6.3).

$$\chi(sl, s'l) = -\frac{\epsilon}{l}\left(2\int_{s'}^{s}\mathcal{A}(s'', s')\,ds'' + B(s')\right)$$

6.2 Green functions equations

For a homogeneous, semi-infinite medium the Green functions equations (5.2) and (5.3) will simplify. The function $A(x) = 0$ and the x-dependence in all parameters vanishes. However, the Green functions $G^{\pm}(x, s, s')$ still are dependent on x, s and s'. The Green functions equations become for $x > 0$, $s > s'$

$$\begin{aligned}\frac{\partial G^+}{\partial x}(x, s, s') &+ \frac{B(x+s') - B(x+s)}{2}G^+(x, s, s') \\ &- \frac{B(x+s)}{2}G^-(x, s, s') - \mathcal{A}(x+s, x+s') \\ &- \int_{s'}^{s}\mathcal{A}(x+s, x+s'')\left(G^+(x, s'', s') + G^-(x, s'', s')\right)ds'' = 0\end{aligned} \tag{6.7}$$

and

$$\begin{aligned}\frac{\partial G^-}{\partial x}(x, s, s') &- 2\frac{\partial G^-}{\partial s}(x, s, s') + \frac{B(x+s)}{2}G^+(x, s, s') \\ &+ \frac{B(x+s') + B(x+s)}{2}G^-(x, s, s') + \mathcal{A}(x+s, x+s') \\ &+ \int_{s'}^{s}\mathcal{A}(x+s, x+s'')\left(G^+(x, s'', s') + G^-(x, s'', s')\right)ds'' = 0\end{aligned} \tag{6.8}$$

with the initial conditions

$$G^-(x, s, s')\big|_{s'=s} = \frac{B(x+s)}{4} \tag{6.9}$$

and

$$G^+(x, s, s')\big|_{s'=s} = \int_0^x\left(\frac{B^2(x'+s)}{8} + \mathcal{A}(x'+s, x'+s)\right)dx' \tag{6.10}$$

This last initial condition follows by integrating (6.7).

The material functions are defined as aforementioned by

$$\begin{cases} B(s) = -\dfrac{l}{\epsilon}\chi(sl, sl) \\ \mathcal{A}(s, s') = -\dfrac{l}{2\epsilon}\dfrac{\partial\chi}{\partial s}(sl, s'l) \end{cases}$$

The boundary values at $x = 0$ ($s > s'$) are

$$\begin{cases} G^+(0, s, s') = 0 \\ G^-(0, s, s') = R(s, s') \end{cases}$$

where $R(s, s')$ is the physical reflection kernel.

6.2.1 Direct algorithm

The direct algorithm based upon the Green functions equations is obtained using similar arguments as in Section 6.1. Integrate the Green functions equations, (6.7) and (6.8), along the characteristics. More explicitly, integrate (6.7) in x from $x-h$ to x and (6.8) from x to $x+h$. The result is

$$\begin{aligned} G^+(x,s,s') = G^+(x-h,s,s') + \int_{x-h}^{x} \Big\{ & \frac{B(x'+s)-B(x'+s')}{2} G^+(x',s,s') \\ & + \frac{B(x'+s)}{2} G^-(x',s,s') + \mathcal{A}(x'+s,x'+s') \\ & + \int_{s'}^{s} \mathcal{A}(x'+s,x'+s'') \left(G^+(x',s'',s') + G^-(x',s'',s') \right) \, ds'' \Big\} \, dx' \end{aligned}$$

and

$$\begin{aligned} G^-(x,s,s') = G^-(x+h,s-2h,s') + \int_{x}^{x+h} \Big\{ & \frac{B(s+2x-x')}{2} G^+(x',s+2x-2x',s') \\ & + \frac{B(x'+s')+B(s+2x-x')}{2} G^-(x',s+2x-2x',s') + \mathcal{A}(s+2x-x',x'+s') \\ & + \int_{s'}^{s+2x-2x'} \mathcal{A}(s+2x-x',x'+s'') \left(G^+(x',s'',s') + G^-(x',s'',s') \right) \, ds'' \Big\} \, dx' \end{aligned}$$

Note that the time s' in these equations is only a parameter. For each value of s' these equations are solved in the domain $0 < x < 1$, $s > s'$.

The discretization mesh in the (x,s)-plane is defined in a similar fashion as before, see Figure 3.

$$(x,s) = (kh,(2i+j)h), \qquad k = 0,1,2,3,\ldots, \quad i = 0,1,2,3,\ldots, \quad j = 0,1,2,3,\ldots$$

Denote the function values as

$$\begin{cases} G^{\pm}_{k,i,j} = G^{\pm}(kh,ih,jh) \\ \mathcal{A}_{i,j} = \mathcal{A}(ih,jh) \\ B_i = B(ih) \end{cases} \quad \text{where} \quad \begin{cases} k = 0,1,2,\ldots,K \\ i = 0,1,2,\ldots,I \\ j = 0,1,2,\ldots,J \end{cases}$$

and approximate all integrals by the trapezoidal rule. The result is

$$\begin{aligned} G^+_{k,i,j} = & G^+_{k-1,i,j} + \frac{h}{2} \Big\{ \frac{B_{k+i}-B_{k+j}}{2} G^+_{k,i,j} + \frac{B_{k+i-1}-B_{k+j-1}}{2} G^+_{k-1,i,j} \\ & + \frac{B_{k+i}}{2} G^-_{k,i,j} + \frac{B_{k+i-1}}{2} G^-_{k-1,i,j} + \mathcal{A}_{k+i,k+j} + \mathcal{A}_{k+i-1,k+j-1} \\ & + \mathcal{P}_{k,i,j} + \mathcal{P}_{k-1,i,j} \Big\} \end{aligned}$$

and

$$\begin{aligned} G^-_{k,i,j} = & G^-_{k+1,i-2,j} + \frac{h}{2} \Big\{ \frac{B_{k+i-1}}{2} G^+_{k+1,i-2,j} + \frac{B_{k+i}}{2} G^+_{k,i,j} \\ & + \frac{B_{k+j+1}+B_{k+i-1}}{2} G^-_{k+1,i-2,j} + \frac{B_{k+j}+B_{k+i}}{2} G^-_{k,i,j} \\ & + \mathcal{A}_{k+i-1,k+j+1} + \mathcal{A}_{k+i,k+j} + \mathcal{P}_{k+1,i-2,j} + \mathcal{P}_{k,i,j} \Big\} \end{aligned}$$

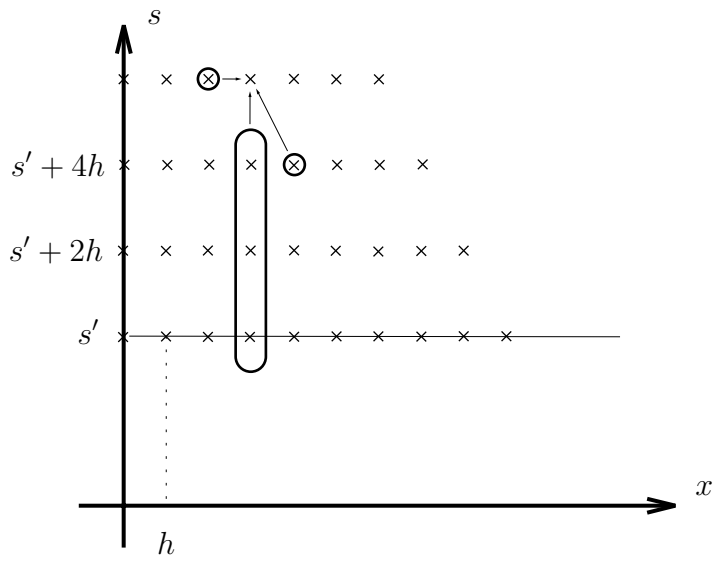

Figure 3: Definition of the mesh in the x-s-plane and the computational molecule of the algorithm based upon the Green functions equation.

where $k = 1, 2, 3, \ldots, K$, $i = j + 2, j + 4, j + 6, \ldots, I$, $j = 0, 1, 2, 3, \ldots, J$ and the convolution term $\mathcal{P}_{k,i,j}$ is defined as

$$\mathcal{P}_{k,i,j} = 2h \sum_{n=0}^{\frac{i-j}{2}}{}''' \mathcal{A}_{k+i,k+j+2n} \left(G^{+}_{k,j+2n,j} + G^{-}_{k,j+2n,j} \right)$$

For $i = j$ the convolution term $\mathcal{P}_{k,i,j}$ is

$$\mathcal{P}_{k,i,i} = 0 \quad , k = 0, 1, 2, 3, \ldots, K$$

The local truncation error made using the trapezoidal rule in the exact expression above is of order $O(h^3)$.

From this discretized version of the Green functions equations the direct scattering algorithm can be derived by solving for $G^{\pm}_{k,i,j}$. The index j in this algorithm is just a parameter. For each $j = 0, 1, 2, 3, \ldots, J$ the direct algorithm requires solution of

$$\begin{cases} A^{11}_{k,i,j} G^{+}_{k,i,j} + A^{12}_{k,i,j} G^{-}_{k,i,j} = F^{1}_{k,i,j} \\ A^{21}_{k,i,j} G^{+}_{k,i,j} + A^{22}_{k,i,j} G^{-}_{k,i,j} = F^{2}_{k,i,j} \end{cases} \tag{6.11}$$

where $k = 0, 1, 2, 3, \ldots, K$, $i = j+2, j+4, j+6, \ldots, I$ and

$$\begin{cases} A^{11}_{k,i,j} = 1 - \dfrac{h}{2}\dfrac{B_{k+i} - B_{k+j}}{2} - \dfrac{h^2}{2}\mathcal{A}_{k+i,k+i} \\ A^{12}_{k,i,j} = -\dfrac{h}{2}\dfrac{B_{k+i}}{2} - \dfrac{h^2}{2}\mathcal{A}_{k+i,k+i} \\ A^{21}_{k,i,j} = -\dfrac{h}{2}\dfrac{B_{k+i}}{2} - \dfrac{h^2}{2}\mathcal{A}_{k+i,k+i} \\ A^{22}_{k,i,j} = 1 - \dfrac{h}{2}\dfrac{B_{k+j} + B_{k+i}}{2} - \dfrac{h^2}{2}\mathcal{A}_{k+i,k+i} \end{cases}$$

The right hand side of (6.11) is

$$\begin{aligned} F^1_{k,i,j} &= G^+_{k-1,i,j} + \frac{h}{2}\Big\{\frac{B_{k+i-1} - B_{k+j-1}}{2}G^+_{k-1,i,j} + \frac{B_{k+i-1}}{2}G^-_{k-1,i,j} \\ &\quad + \mathcal{A}_{k+i,k+j} + \mathcal{A}_{k+i-1,k+j-1} + \mathcal{P}'_{k,i,j} + \mathcal{P}_{k-1,i,j}\Big\} \\ F^2_{k,i,j} &= G^-_{k+1,i-2,j} + \frac{h}{2}\Big\{\frac{B_{k+i-1}}{2}G^+_{k+1,i-2,j} + \frac{B_{k+j+1} + B_{k+i-1}}{2}G^-_{k+1,i-2,j} \\ &\quad + \mathcal{A}_{k+i-1,k+j+1} + \mathcal{A}_{k+i,k+j} + \mathcal{P}'_{k,i,j} + \mathcal{P}_{k+1,i-2,j}\Big\} \end{aligned}$$

and the truncated convolution term is

$$\mathcal{P}'_{k,i,j} = 2h \sum_{n=0}^{\frac{i-j-2}{2}}{}' \mathcal{A}_{k+i,k+j+2n}\left(G^+_{k,j+2n,j} + G^-_{k,j+2n,j}\right)$$

From equation (6.11) it is straightforward to calculate the $G^{\pm}_{k,i,j}$ as functions of known quantities. The initial values of the Green functions are, see (6.9) and (6.10),

$$\begin{cases} G^-_{k,j,j} = \dfrac{B_{k+j}}{4} \\ G^+_{k,j,j} = h \displaystyle\sum_{n=0}^{k}{}''' \left(\frac{B^2_{n+j}}{8} + \mathcal{A}_{n+j,n+j}\right) \end{cases}$$

and the boundary values of the Green functions at $x = 0$ are

$$\begin{cases} G^+_{0,i,j} = 0 \\ G^-_{0,i,j} = R_{i,j} \end{cases}$$

The boundary value $G^+_{0,i,j}$ is exact and the values of $G^-_{0,i,j} = R_{i,j}$ are the sought quantities of the direct algorithm. Note that the matrix on the left hand side in (6.11), i.e.,

$$\begin{pmatrix} A^{11}_{k,i,j} & A^{12}_{k,i,j} \\ A^{21}_{k,i,j} & A^{22}_{k,i,j} \end{pmatrix}$$

is non-singular for sufficiently small step size h. The algorithm starts from the horizontal line $i = j$, where the initial values of the Green functions are known

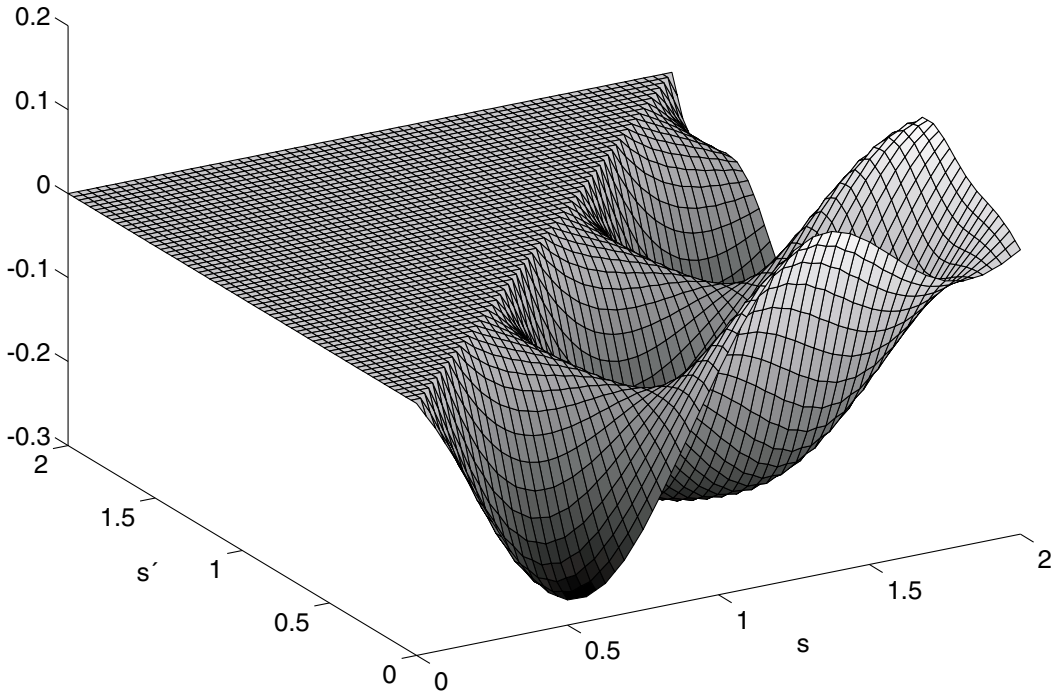

Figure 4: The reflection kernel $R(s, s')$ corresponding to the medium in (7.1).

and proceeds to higher i-values, on each line i = constant calculating the Green functions from the left to the right. This is the direct numerical algorithm for the computation of the Green functions.

Despite the fact that the Green functions algorithm developed in this section contains less numerical integration when compared to the imbedding approach which was developed in Section 6.1, the latter one is faster. This is due to the fact that the reflection kernel in the imbedding approach is only a function of two arguments, but the Green functions are functions of three variables. The s' coordinate in the Green functions method is a parameter, and for each value of s' a new direct problem has to be solved. The reflection kernel is obtained as boundary values at $x = 0$ of the Green functions. However, the more complex calculations that occur in the Green function approach also provide the internal field of the medium, whereas the imbedding approach lacks this property.

7 Numerical examples

The analysis developed in this paper is illustrated with some numerical computations of model problems.

The direct scattering problem is solved using the Green function approach de-

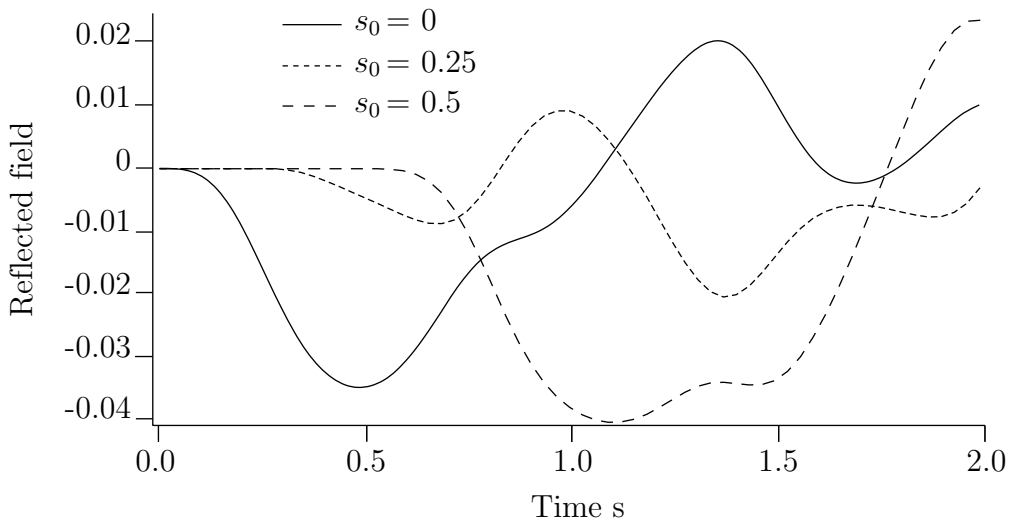

Figure 5: The amplitude of the reflected field $u^-(0,s)$ for three different delayed excitations, $u^+(0,s) = H(s-s_0)\sin\omega(s-s_0)$ for $\omega = 10$.

scribed in Section 6.2.1. The reconstruction of the susceptibility kernel, however, is made using the inverse scattering algorithm based upon the imbedding method developed in Section 6.1.2. The reason for using two different numerical algorithms in the solution of the direct and the inverse scattering problems, is to avoid any reconstruction bias. Two model problems and the corresponding reconstructions of noise-less data are presented.

Example 1: This model is a generalized resonance model. The susceptibility kernel $\chi(t,t')$, which is discussed further in Appendix B, is

$$\begin{cases} \epsilon = 1 \\ \chi(sl, s'l) = \dfrac{\omega_p^2(sl)}{\nu_0} e^{-\nu(sl-s'l)/2} \sin \nu_0(sl - s'l) \end{cases}$$

In Figure 4 the reflection kernel corresponding to the medium

$$\chi(sl, s'l) = (1 + .4\sin 10s)^2 e^{-.5(s-s')} \sin 2(s-s') \tag{7.1}$$

is depicted.

To illustrate how the reflected field $u^-(0,s)$ is affected by different excitations, the medium is excited by a delayed sinusoidal wave.

$$u^+(0,s) = H(s-s_0)\sin\omega(s-s_0)$$

The effect on the reflected field for three different delay factors s_0 is computed in Figure **??**. Large variations in the response of the medium are found, so illustrating the medium is far from being time translation invariant.

The reconstruction of the medium using the inverse algorithm (6.6) is depicted in Figure 6. The relative error is always less than 1% in this reconstruction using a 64×64 mesh in (s, s').

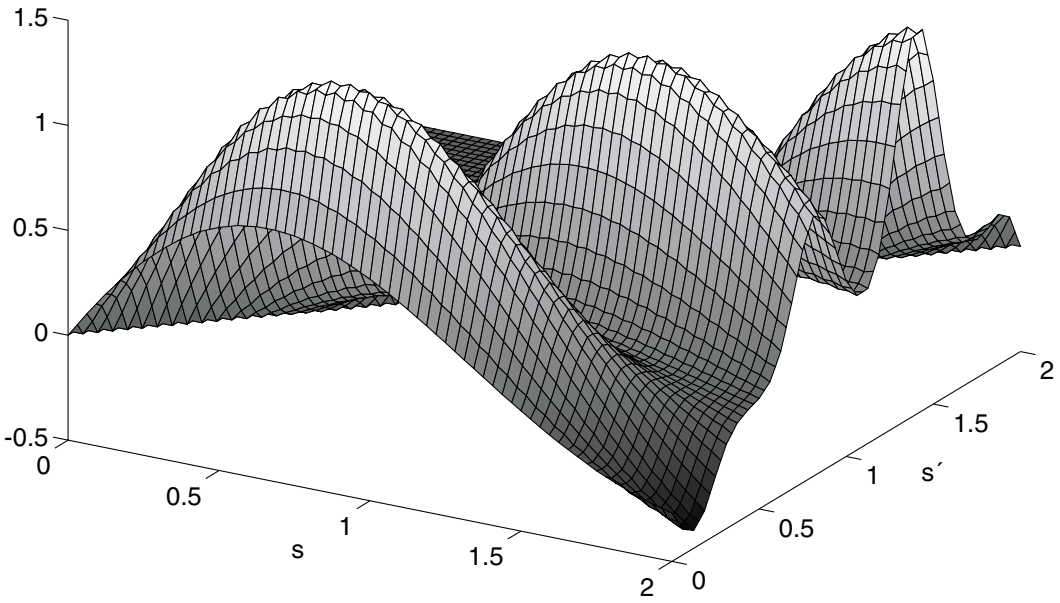

Figure 6: The reconstructed susceptibility kernel $\chi(sl, s'l)$ in (7.1).

Example 2: The second example illustrates a generalized Debye model in which the relaxation time τ is allowed to vary with time, see Appendix C. The susceptibility kernel used in this example is,

$$\chi(sl, s'l) = 2 \exp\left\{ - \int_{s'}^{s} \frac{ds''}{\tau(s'')} \right\} \tag{7.2}$$

where the relaxation time changes from τ_1 to τ_2 as

$$\frac{1}{\tau(s)} = \begin{cases} \frac{1}{\tau_1}, & 0 \le s \le s_1 \\ \frac{\tau_1+\tau_2}{2\tau_1\tau_2} - \frac{\tau_1-\tau_2}{2\tau_1\tau_2} \cos \pi \frac{s-s_1}{s_2-s_1}, & s_1 \le s \le s_2 \\ \frac{1}{\tau_2}, & s_2 \le s \le 2 \end{cases}$$

A reconstruction of an explicit example is depicted Figure 7, where $\tau_1 = 1$, $\tau_2 = 6$, $s_1 = .9$ and $s_2 = 1.4$. The relative error in this reconstruction is less than 0.3% using a 64×64 mesh in (s, s').

8 Summary

In this paper new equations for the reflection kernel and the Green functions have been derived, when the medium is such that the solutions to the differential equations

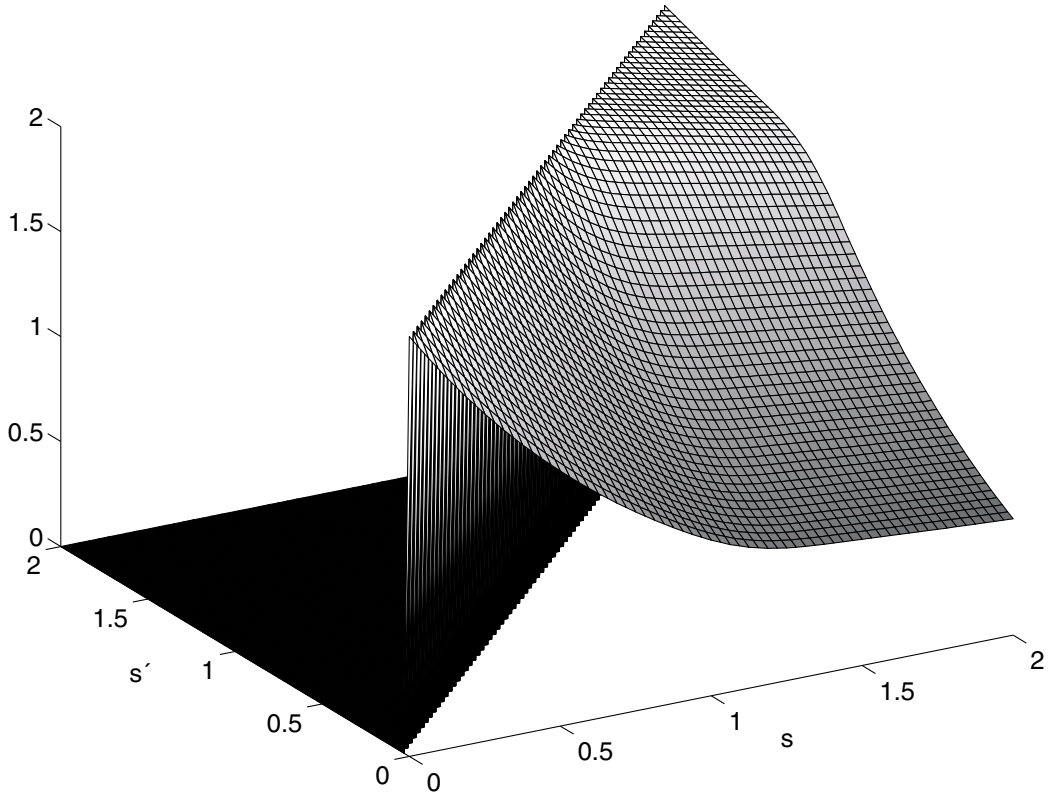

Figure 7: The reconstructed susceptibility kernel $\chi(sl, s'l)$ in (7.2).

do not admit time translation. It is also shown in Appendix A that these new equations reduce to the well known equations when the medium *does* admit time translation invariance.

For the special case of a semi-infinite medium, where the material has no spatial dependence, it is shown that the functional equations are only functions of two independent variables. For this more tractable problem, a few computational examples for the direct and inverse problem illustrate the method.

Extensions of these methods to more general problems will be reported elsewhere.

Acknowledgment

One of the authors (G.K.) wishes to express his gratitude to the Department of Mathematics, University of Canterbury, Christchurch, New Zealand for the Visiting Erskine Fellowship that initiated this project and collaboration. The work reported in this paper is partially supported by a grant from the Swedish Research Council for Engineering Sciences and their support is gratefully acknowledged.

Appendix A Invariance under time translations

In this appendix it is shown that the equations of Sections 4 and 5 reduce to those to be found in previous literature [1, 3, 6, 11] when the medium is *assumed* to admit time translation invariance.

If the medium is invariant under time translations, the susceptibility kernel $\chi(z,t,t')$ is only a function of z and the difference $t-t'$. This implies that the reflection kernel $R(x,s,s')$ also is only a function of x and $s-s'$ and the imbedding equation for $R(x,s)$ satisfies ($0<x<1,\ s>0$)

$$\begin{aligned}\frac{\partial R}{\partial x}(x,s)-2\frac{\partial R}{\partial s}(x,s) &= -\frac{A(x)}{2}\int_0^s R(x,s-s')R(x,s')\,ds' \\ &\quad -\frac{\partial}{\partial s}\Big\{\frac{1}{2}D(x,s)+\int_0^s R(x,s-s')D(x,s')\,ds' \\ &\quad +\frac{1}{2}\int_0^s R(x,s-s')\int_0^{s'} D(x,s'-s'')R(x,s'')\,ds''\,ds'\Big\}\end{aligned}$$

with the initial condition

$$R(x,0)=-\frac{A(x)-B(x)}{4}$$

The functions $A(x)$ and $B(x)$ and $D(x,s)$ have in this appendix slightly different definitions compared to the definitions in the main sections in this paper.

$$\begin{cases} A(x)=\dfrac{1}{2}\dfrac{\mathrm{d}}{\mathrm{d}x}\ln\epsilon(z(x)) \\ B(x)=-\dfrac{l}{\epsilon(z(x))}\chi(z(x),0) \\ D(x,s)=-\dfrac{l}{\epsilon(z(x))}\chi(z(x),sl) \end{cases}$$

Note the difference in the definition of the function $D(x,s)$ and the definition of the function $D(x,s,s')$ in (2.4).

The finite jump discontinuity of the reflection kernel is

$$\begin{aligned}[R(x,2(1-x))] &= [R(1,0)]\exp\left\{\int_x^1 B(x')\,dx'\right\} \\ &= \frac{A(1^-)-B(1^-)}{4}\exp\left\{\int_x^1 B(x')\,dx'\right\}\end{aligned}$$

where square brackets are used to denote the finite jump discontinuity, i.e.,

$$[R(x,s)]=R(x,s^+)-R(x,s^-)$$

The Green functions equations simplify in a similar fashion for a time invariant medium. The Green functions are also functions of just two arguments, x and $s-s'$.

The Green functions equations $G^{\pm}(x,s)$ satisfy $(0<x<1,\ s>0)$

$$2\frac{\partial G^+}{\partial x}(x,s) = A(x)G^-(x,s) - B(x)G^+(x,s) + \frac{\partial}{\partial s}\left\{D(x,s) + \int_0^s D(x,s-s')\left(G^+(x,s') + G^-(x,s')\right)\,ds'\right\}$$

and

$$2\frac{\partial G^-}{\partial x}(x,s) - 4\frac{\partial G^-}{\partial s}(x,s) = A(x)G^+(x,s) - B(x)G^-(x,s) - \frac{\partial}{\partial s}\left\{D(x,s) + \int_0^s D(x,s-s')\left(G^+(x,s') + G^-(x,s')\right)\,ds'\right\}$$

where the same definitions of the functions $A(x)$, $B(x)$ and $D(x,s)$ as above have been used. The initial condition is

$$G^-(x,0) = -\frac{A(x)-B(x)}{4}$$

Appendix B Resonance model

The polarization vector, $\boldsymbol{P}(\boldsymbol{r},t)$, is assumed to satisfy the following dynamics at each space point:

$$\frac{\mathrm{d}^2\boldsymbol{P}}{\mathrm{d}t^2}(t) + \nu(t)\frac{\mathrm{d}\boldsymbol{P}}{\mathrm{d}t}(t) + \omega_0^2(t)\boldsymbol{P}(t) = \epsilon_0\omega_p^2(t)\boldsymbol{E}(t)$$

This is a generalized resonance (Lorentz) model in which the collision frequency $\nu(t)$, the resonance frequency $\omega_0(t)$ and the plasma frequency $\omega_p(t)$ are allowed to vary with respect to time. The constitutive relations, given by (2.2), are used to rewrite this equation as an initial value problem for the susceptibility kernel $\chi(t,t')$. The result is

$$\begin{cases} \epsilon = 1 \\ 2\left.\dfrac{\partial\chi}{\partial t}(t,t')\right|_{t'=t} + \left.\dfrac{\partial\chi}{\partial t'}(t,t')\right|_{t'=t} = \omega_p^2(t) \\ \chi(t,t) = 0 \\ \dfrac{\partial^2\chi}{\partial t^2}(t,t') + \nu(t)\dfrac{\partial\chi}{\partial t}(t,t') + \omega_0^2(t)\chi(t,t') = 0 \end{cases}$$

The solution to this problem for constant collision frequency ν and the resonance frequency ω_0 is

$$\begin{cases} \epsilon = 1 \\ \chi(t,t') = \dfrac{\omega_p^2(t)}{\nu_0}e^{-\nu(t-t')/2}\sin\nu_0(t-t') \end{cases}$$

where

$$\nu_0 = \sqrt{\omega_0^2 - \nu^2/4}$$

Appendix C Debye model

In this model, the underlying dynamics of the polarization vector is assumed to satisfy, see also Ref. [6]

$$\frac{\mathrm{d}\boldsymbol{P}}{\mathrm{d}t}(t) = \epsilon_0 \alpha(t) \boldsymbol{E}(t) - \frac{1}{\tau(t)} \boldsymbol{P}(t)$$

at each point in space. The first term on the right hand side is the term responsible for the alignment effects in the medium, while the second models the effect of random order. The relaxation τ and the alignment frequency α are assumed to be time varying. The constitutive relations, given by (2.2), imply that the following relations hold:

$$\begin{cases} \epsilon = 1 \\ \chi(t,t) = \alpha(t) \\ \dfrac{\partial \chi}{\partial t}(t,t') + \dfrac{1}{\tau(t)} \chi(t,t') = 0 \end{cases}$$

The solution to these equations is

$$\begin{cases} \epsilon = 1 \\ \chi(t,t') = \alpha(t') \exp\left\{ - \displaystyle\int_{t'}^{t} \frac{dt''}{\tau(t'')} \right\} \end{cases}$$

References

[1] R.S. Beezley and R.J. Krueger. An electromagnetic inverse problem for dispersive media. *J. Math. Phys.*, **26**(2), 317–325, 1985.

[2] D. Colton, R. Ewing, and W. Rundell, editors. *Inverse Problems in Partial Differential Equations*. SIAM, 1990.

[3] J.P. Corones, M.E. Davison, and R.J. Krueger. Direct and inverse scattering in the time domain via invariant imbedding equations. *J. Acoust. Soc. Am.*, **74**(5), 1535–1541, 1983.

[4] J.P. Corones, M.E. Davison, and R.J. Krueger. Wave splittings, invariant imbedding and inverse scattering. In A.J. Devaney, editor, *Inverse Optics*, pages 102–106, SPIE Bellingham, WA, 1983. Proc. SPIE 413.

[5] J.P. Corones, G. Kristensson, P. Nelson, and D.L. Seth, editors. *Invariant Imbedding and Inverse Problems*. SIAM, 1992.

[6] G. Kristensson. Direct and inverse scattering problems in dispersive media—Green's functions and invariant imbedding techniques. In Kleinman R., Kress R., and Martensen E., editors, *Direct and Inverse Boundary Value Problems*, Methoden und Verfahren der Mathematischen Physik, Band 37, pages 105–119, Mathematisches Forschungsinstitut Oberwolfach, FRG, 1991.

[7] G. Kristensson and R.J. Krueger. Direct and inverse scattering in the time domain for a dissipative wave equation. Part 1: Scattering operators. *J. Math. Phys.*, **27**(6), 1667–1682, 1986.

[8] G. Kristensson and R.J. Krueger. Direct and inverse scattering in the time domain for a dissipative wave equation. Part 2: Simultaneous reconstruction of dissipation and phase velocity profiles. *J. Math. Phys.*, **27**(6), 1683–1693, 1986.

[9] G. Kristensson and R.J. Krueger. Direct and inverse scattering in the time domain for a dissipative wave equation. Part 3: Scattering operators in the presence of a phase velocity mismatch. *J. Math. Phys.*, **28**(2), 360–370, 1987.

[10] G. Kristensson and R.J. Krueger. Direct and inverse scattering in the time domain for a dissipative wave equation. Part 4: Use of phase velocity mismatches to simplify inversions. *Inverse Problems*, **5**(3), 375–388, 1989.

[11] R.J. Krueger and R.L. Ochs, Jr. A Green's function approach to the determination of internal fields. *Wave Motion*, **11**, 525–543, 1989.

[12] L.P. Nizhnik. Inverse problem of nonstationary scattering. *Soviet Math. Dokl.*, **12**(1), 306–310, 1971.

[13] L.P. Nizhnik. The inverse scattering problems for the hyperbolic equations and their application to non-linear integrable systems. *Reports on Mathematical Physics*, **26**(2), 261–283, 1988.

[14] L.P. Nizhnik and V.G. Tarasov. The inverse scattering problems for an integrodifferential equation. *Selecta Mathematica Sovietica*, **10**(3), 219–236, 1991.

[15] L. Päivärinta and E. Somersalo, editors. *Inverse Problems in Mathematical Physics*. Springer-Verlag, Berlin, 1993.

[16] Kleinman R., Kress R., and Martensen E., editors. *Direct and Inverse Boundary Value Problems*. Methoden und Verfahren der Mathematischen Physik, Band 37. Peter Lang, Frankfurt am Main, 1991.

[17] V.H. Weston. Invariant imbedding for the wave equation in three dimensions and the applications to the direct and inverse problems. *Inverse Problems*, **6**, 1075–1105, 1990.

[18] V.H. Weston. Invariant imbedding and wave splitting in $\mathbf{R}^3$: II. the Green function approach to inverse scattering. *Inverse Problems*, **8**, 919–947, 1992.